frontiers | Frontiers in Immunology

TYPE Original Research
PUBLISHED 24 October 2024
DOI 10.3389/fimmu.2024.1480041

OPEN ACCESS

EDITED BY
Julie Olson,
University of Minnesota Twin Cities, United States

REVIEWED BY
Joel Wilmore,
Upstate Medical University, United States
Rosangela Salerno-Goncalves,
University of Maryland, United States

*CORRESPONDENCE
Tomas Strandin
tomas.strandin@helsinki.fi

RECEIVED 13 August 2024
ACCEPTED 08 October 2024
PUBLISHED 24 October 2024

CITATION
Cabrera LE, Buckner C, Then V, Mäki S, Vapalahti O, Vaheri A, Hepojoki J, Tietäväinen J, Mäkelä S, Mustonen J and Strandin T (2024) Circulating mucosal-like IgA responses increase with severity of Puumala orthohantavirus-caused hemorrhagic fever with renal syndrome.
Front. Immunol. 15:1480041.
doi: 10.3389/fimmu.2024.1480041

Circulating mucosal-like IgA responses increase with severity of Puumala orthohantavirus-caused hemorrhagic fever with renal syndrome

Luz E. Cabrera[1], Cienna Buckner[1], Veronica Then[1], Sanna Mäki[1], Olli Vapalahti[1], Antti Vaheri[1], Jussi Hepojoki[1], Johanna Tietäväinen[2,3], Satu Mäkelä[2,3], Jukka Mustonen[2,3] and Tomas Strandin[1]*

[1]Viral Zoonosis Research Unit, Department of Virology, Medicum, University of Helsinki, Helsinki, Finland, [2]Faculty of Medicine and Health Technology, Tampere University, Tampere, Finland, [3]Department of Internal Medicine, Tampere University Hospital, Tampere, Finland

Old World Orthohantaviruses cause hemorrhagic fever with renal syndrome (HFRS) characterized by increased vascular permeability and acute kidney injury (AKI). Despite the systemic nature of the disease, the virus enters humans through inhalation and therefore initially encounters the immunoglobulin class A (IgA) dominated mucosal immune system. Herein, we characterized systemic IgA responses and their potential relationship to the mucosal immune activation by examining blood samples obtained from patients hospitalized due to acute Puumala orthohantavirus infection. Our findings reveal increased frequencies of putative IgA-expressing circulating mucosal-associated B1 cells and plasmablasts, as well as elevated levels of polyreactive, polymeric, virus-specific and secretory IgA in the acute stage of the disease. Importantly, the levels of circulating virus-specific and secretory IgA, as well as the putative IgA+ B1 cells, increased with the severity of AKI. Furthermore, circulating polymeric IgA displayed enhanced effector functions by forming stable complexes with the IgA receptor CD89 and induced pro-inflammatory neutrophil responses. These results suggest that excessive levels of circulating mucosal-like IgA might serve as a biomarker for HFRS disease progression.

KEYWORDS

HFRS, hantavirus, IgA, mucosal immunity, neutrophils

Introduction

Orthohantaviruses endemic in Europe and Asia cause hemorrhagic fever with renal syndrome (HFRS), whereas the viruses present in the Americas cause hantavirus cardiopulmonary syndrome (HCPS) (1). Puumala orthohantavirus (PUUV) is the most prevalent orthohantavirus in Europe and carried by the bank vole (Myodes glareolus). When transmitted from rodent excretions to humans, it causes a relatively mild form of HFRS (PUUV-HFRS), the typical symptoms of which include fever, vomiting, diarrhea, headache, backache and myopia (2). Hospitalized PUUV-HFRS patients often present with acute kidney injury (AKI), the molecular mechanisms of which remain unclear. Increased vascular permeability due to the loss of endothelial cell (EC) barrier functions is pathognomonic to orthohantavirus-mediated diseases, including PUUV-HFRS. Virus replication occurs primarily in the capillary ECs but is without direct cytopathic effects and thus does not directly explain the increased vascular permeability (3, 4). In fact, it is generally believed that aberrant immunological responses towards the virus play a major role in the development of HFRS (5). However, the lack of an animal disease model greatly hampers the detailed pathogenesis investigations for HFRS (6).

The virus infection occurs through inhalation (1), which suggests that the mucosal immune system of the airways is the first to respond to the infection. Furthermore, HFRS symptoms include vomiting and diarrhea (2), which implies the involvement of the gastrointestinal tract that harbors the largest mucosal immune compartment in humans. Mucosal immunity is largely mediated by IgA, the most abundant antibody isotype in humans. A major proportion of IgA is produced by mucosal tissue resident plasma cells in the lamina propria, from where it migrates through transepithelial transport to the luminal space of the mucosal tissue (7). During the transport, the secretory component (SC) is covalently linked to IgA, allowing the distinction of secretory IgA (sIgA) from the other IgA forms. The mucosal IgA is distinct from systemic circulating IgA due to its propensity to form dimers or polymers (8) and its ability to bind multiple antigens simultaneously (i.e. polyreactivity) (9).

The trafficking of antibody secreting cells (ASCs) to the intestine is mediated by their expression of the homing receptors α4β7 integrin (10) and C-C Chemokine receptor type 9 (CCR9) (11), with the latter being responsible for homing specifically to the small intestine. The fast-responding and rigorously IgA expressing intestinal plasma cells are further characterized by their expression of integrin CD11b (12). In addition to plasmablasts (PBs) and plasma cells, B1 cells are another class of fast-responding ASCs (13). Originally discovered in the peritoneal cavity of mice, B1 cells are innate-like cells that spontaneously release antibodies (abs) with minimal somatic hypermutation, producing natural abs distinct from the high-affinity abs produced by plasma cells. While the exact phenotype of human B1 cells has been a topic of debate (14), Quach et al. were able to reliably discriminate B1 cells from other ASCs as $CD20^{+}CD27^{+}CD38^{-/int}CD43^{+}CD70^{-}$ (15). Interestingly, in response to infection, B1 cells migrate to the lymph nodes through increased expression of CD11b (16).

We recently observed increased frequencies of IgA-expressing PBs in the circulation of acute PUUV-HFRS (17). However, the role of IgA in the development of PUUV-HFRS is not well understood. In the current study, we aimed to gain a deeper view of the IgA-dominated mucosal immunity activation in HFRS by analyzing mucosal homing receptor expression of IgA ASCs and assessing mucosal-associated IgA levels in the circulation during acute, convalescent and recovery stage PUUV-HFRS. Furthermore, we studied the potential pathologic and pro-inflammatory roles of circulating IgA during the disease.

Materials and methods

Patient population

The study material consisted of serum and PBMCs from serologically-confirmed PUUV-infected patients hospitalized (Tampere University Hospital, Finland) between 2005 and 2009. The patient samples were systematically collected from a cohort of 55 individuals (or 25 in case of PBMCs), at different time points, which included the acute phase for samples taken during hospitalization (5-9 days after onset of fever {aof}), the postacute/convalescent phase for samples taken 14 days after discharge from hospital (~30 days aof), and the recovery phase for samples taken 6 months and one year aof. The recovery samples served as steady state controls. The study protocol was approved by the Ethical Committee of Tampere University Hospital with permit number R04180.

Standard methods were employed to determine daily white blood cell (WBC) and thrombocyte count, plasma C-reactive protein (CRP), and serum creatinine concentrations at the Laboratory Centre of the Pirkanmaa Hospital District (Tampere, Finland). Descriptive patient characteristics are given in Table 1.

PBMC analysis by flow cytometry

Frozen PUUV patient PBMCs were thawed in a 37°C water bath for 5 min and washed with R10 (RPMI-1640 (Sigma Aldrich) supplemented with 10% inactivated FCS (Gibco), 100 IU/ml of penicillin (Sigma Aldrich), 100 µg/ml of streptomycin (Sigma Aldrich) and 2 mM of L-glutamine (Sigma Aldrich)) and including 100 µg/ml DNAse I (Sigma Aldrich). After a 10 min incubation at RT, the cells were washed once with the R10 and once with PBS-EDTA (PBS with 2 mM EDTA), followed by cell quantification using Bio-Rad cell counter TC20.

One to three million PBMCs were incubated in 1% FCS and FcR blocking reagent (BioLegend), and the cells stained for 30 min at RT with a cocktail of fluorescent dye conjugated anti-human mouse monoclonal antibodies recognizing cell surface antigens(the antibody panel is provided in detail in Table 2) and a live/dead fixable green dead cell marker (Thermo Fisher). After staining, the cells were washed once with PBS-EDTA and fixed with 1%

10.3389/fimmu.2024.1480041

TABLE 1 Clinical and laboratory data during hospitalization in patients with acute PUUV infection.

Parameter (unit)	Range (Median± IQR) Serum (n = 55)	Range (Median + IQR) PBMCs (n = 25)	Reference value
Age (years)	22 – 74 (39 ± 19)	25 – 67 (35 ± 22)	–
Gender (Male: Female)	33:22	15:10	–
Duration of fever (days)	3 – 15 (8 ± 3)	3 – 9 (7 ± 2)	–
Length of hospital stay (days)	2 – 25 (5 ± 3)	2 – 25 (5 ± 2)	_
Max Creatinine (µmol/L)	51 – 1499 (165 ± 376)	51 – 1499 (150 ± 279)	Male: 62 – 115/Female: 53 – 97
Max WBC (E9/L)	6 – 26 (10 ± 5)	7 – 26 (11 ± 5)	3.4 – 8.2
Min Thrombocytes (E9/L)	15 – 118 (54 ± 41)	15 – 118 (61 ± 44)	150 – 360
Max C-reactive protein (mg/L)	16 – 267 (91 ± 67)	16 – 267 (89 ± 92)	< 4

WBC, white blood cells; IQR, Interquartile range.

paraformaldehyde before FACS analysis with a 4-laser (405, 488, 561 and 637 nm) Quanteon Novocyte (Agilent Technologies).

Neutrophil analysis by flow cytometry

Neutrophils were isolated from EDTA-anticoagulated blood of healthy controls using Polymorphprep (Proteogenix) and $2*10^6$/ml neutrophils in R10 were incubated with 10 µg/ml IgA in 10 µl for 4 hours at 37°C. Samples were then incubated with CellROX green dye (Thermo Fisher) and an antibody cocktail (Table 3) for 30min at RT. Finally, the samples were diluted 1:20 in PBS and analyzed using a BD Fortessa LSRII flow cytometry (BD Biosciences).

TABLE 2 PBMC flow cytometry antibody panel.

Marker	Fluorochrome	Clone	Company
CD3	FITC	OKT3	ThermoFisher
CD14	FITC	MEM-18	Immunotools
CD56	FITC	MEM-188	Immunotools
CD66	FITC	6g5j	Immunotools
α4β7	PE	Hu117	RnD Systems
IgA	PE-Cy7	IS11-8E10	MACS Miltenyi
CD43	PerCP-efluor 710	4-29-5-10-21	ThermoFisher
CCR9	APC	L053E8	Biolegend
IgD	APC-Cy7	IA6-2	Biolegend
CD38	BV421	HB7	Biolegend
CD19	BV510	SJ25C1	Biolegend
CD11b	BV605	ICRF44	BD Biosciences
CD27	BV711	M-T271	Biolegend
CD70	BV786	Ki-24	BD Biosciences
CD20	BB615	2H7	Bio-Rad

PBMC cultures

Frozen patient PBMCs were revived similarly as described for flow cytometry above. PBMCs (at 1 million/ml) were cultured in R10 for 6 days at 37°C, centrifuged for 10 min at 400 g and supernatants collected for ELISA as specified below. The extended culturing period of 6 days was chosen to ensure highest possible amount of spontaneously produced antibodies, including less frequent antibody types (18). However, the extended culturing period may have its limitations such as non-spontaneous antibody release from dying/dead cells, which was not addressed in our study.

ELISAs

The amounts of IgA and sIgA were measured by ELISA protocols including capture mAbs anti-human IgA (clone MT57, Mabtech) for IgA and anti-human secretory component (clone SC-05, Exbio) for sIgA. Capture mAbs were coated onto MaxiSorp plates (ThermoFisher) at 2 µg/ml in PBS overnight in +4°C and blocked with 1% BSA-PBS for 1 hr prior to incubating with diluted patient serum, PBMC supernatant or isolated IgA samplesas detailed in figure legends for 1 hr. After washing with PBS containing 0.05% Tween-20 (PBST), the plates were incubated with Horseradish peroxidase (HRP, Dako, dilution 1:6000)- or alkaline phosphatase (ALP, clone MT20, Mabtech, dilution 1:1000)-conjugated secondary IgA-specific antibodies for IgA and sIgA. After washing with PBST, the HRP- and ALP-conjugated Abs were detected by 3,3′,5,5′-tetramentylbenzidine (TMB) or para-nitrophenyl phosphate (pNPP) substrates, respectively (Thermo Scientific). TMB-mediated reaction was stopped by addition of

10.3389/fimmu.2024.1480041

TABLE 3 Neutrophil flow cytometry antibody panel.

Marker	Fluorochrome	Clone	Company
LOX-1	PE	15C4	BioLegend
IgA	PE-Cy7	IS11-8E10	MACS Miltenyi
CD11b	APC-Cy7	ICRF44	Biolegend
CD66b	BV421	G10F5	BD Biosciences
CD62L	BV605	DREG-56	BD Biosciences
HLA-DR	BV786	G46-6	BD Biosciences

0.5 M H_2SO_4. Absorbances (450 nM for HRP- and 405 nM for ALP-based reactions) were read by HIDEX sense microplate reader. As standards, native human IgA from Mabtech and sIgA isolated from healthy donor saliva were used. To detect virus-specific, polyreactive or receptor binding of IgA, the capture antibodies were replaced by baculovirus-expressed PUUV nucleocapsid (N) protein (2 µg/ml), DNP-conjugated albumin (10 µg/ml, Sigma) or CD89 (2 µg/ml, RnD systems), respectively.

IgA isolations

IgA was isolated from serum using peptide M agarose following manufacturer's recommendations (Invivogen). The isolated IgAs were eluted into 10 mM Glycine pH 1.7, followed by buffer exchange to PBS and sample concentration using 50 kDa centrifugal filters (Amicon, Millipore). Approximately 1 mg of isolated IgAs were separated into polymeric, dimeric and monomeric fractions by size-exclusion chromatography (Sephadex G-200) using Äkta HPLC (Cytiva), fractions concentrated using 50 kDa centrifugal filters and analyzed by ELISA.

Binding kinetics

The binding of IgA to CD89 was analyzed with surface plasmon resonance with Biacore T100 instrumentation (Cytiva). The flow cells of a CM5 S series biosensor chip (Cytiva) were covalently coated with CD89 via standard amine coupling or left empty (negative control). The coating with CD89 resulted in a resonance unit (RU) increase of approximately 1000. The binding was analyzed using PBS as the running buffer and a flow rate of 20 µL min–1. The kinetics of the IgA binding to CD89 were measured by varying IgA concentrations with a contact time of 2 min and a dissociation phase of 10 min. After the completion of the dissociation phase, the flow cells were regenerated with 10 mM Glycine, pH 1.7. The data were evaluated by first subtracting the sensorgrams obtained from empty negative control flow cell from those obtained from the flow cells containing CD89. Association and dissociation rate constants were obtained by the Langmuir global fit model (BiaEvaluation Software, Cytiva).

On cell-ELISA

Blood microvascular endothelial cells (BECs) were obtained from Lonza and maintained in endothelial basal medium (EBM-2) supplemented with SingleQuots™ Kit containing 5% fetal bovine serum (FBS), human endothelial growth factor, hydrocortisone, vascular endothelial growth factor, human fibroblast growth factor-basic, ascorbic acid, R3-insulin like growth factor-1, gentamicin and amphotericin-B (Lonza). The experiments were performed on cells at passage 7 or 8. Isolated IgAs at 10 µg/ml were incubated with BECs for 45 min on ice, after which cells were washed with PBS 3 times and fixed with 4% paraformaldehyde for 10 min at RT. Fixed cells were blocked with 1% BSA-PBS for 30 min at RT and incubated with HRP-conjugated polyclonal anti-human IgA (1:6000, Dako) for 1 hr and washed with PBS 3 times. Color was developed with TMB and reaction stopped with 0.5 M H_2SO_4. Absorbance at 450nm was read by HIDEX sense microplate reader.

Statistical analyses

Statistically significant differences between time points were assessed by generalized estimating equations with working correlation matrix set as independent and gamma with log link scale response as the model (SPSS v29). Generalized estimating equations is a computationally simple method to analyze longitudinal data and has the ability to account for missing data points (19, 20). The results of generalized estimating equations are shown in Supplementary File 1. Grouped non-parametric patient data was analyzed Mann-Whitney test and differences between treatment groups were analyzed by two-way ANOVA using Tukey's test for multiple comparisons using GraphPad Prism (v8). All reported p-values are two-sided with the minimum threshold used for statistical significance set at $p < 0.05$.

Results

IgA-expressing B cellsare significantly increased during acute PUUV-HFRS

We previously identified significantly increased frequencies of IgA-expressing PBs in the peripheral blood during acute PUUV-HFRS (17). To understand the tissue tropism of these PBs, we developed an assay to measure the surface expression of mucosal homing receptors integrin α4β7, CD11b, and CCR9 in virus-induced PBs, using multicolor flow cytometry. Alongside PBs ($CD20^{\pm}$ $CD19^{+}IgD^{-}CD27^{+}CD38^{++}CD43^{+}$), we investigated the frequencies and IgA expression of the putative mucosal-associated B1 cells in the circulation. The exact identity of human B1 cells is still controversial and standard phenotypic markers to identify human B1 have not yet been established. For this study, we decided to use the phenotype described by Quach et al. ($CD20^{+}CD19^{+}CD27^{+}CD38^{-/int}CD43^{+}CD70^{-}$, representative gating strategy shown in Supplementary Figure 1).

10.3389/fimmu.2024.1480041

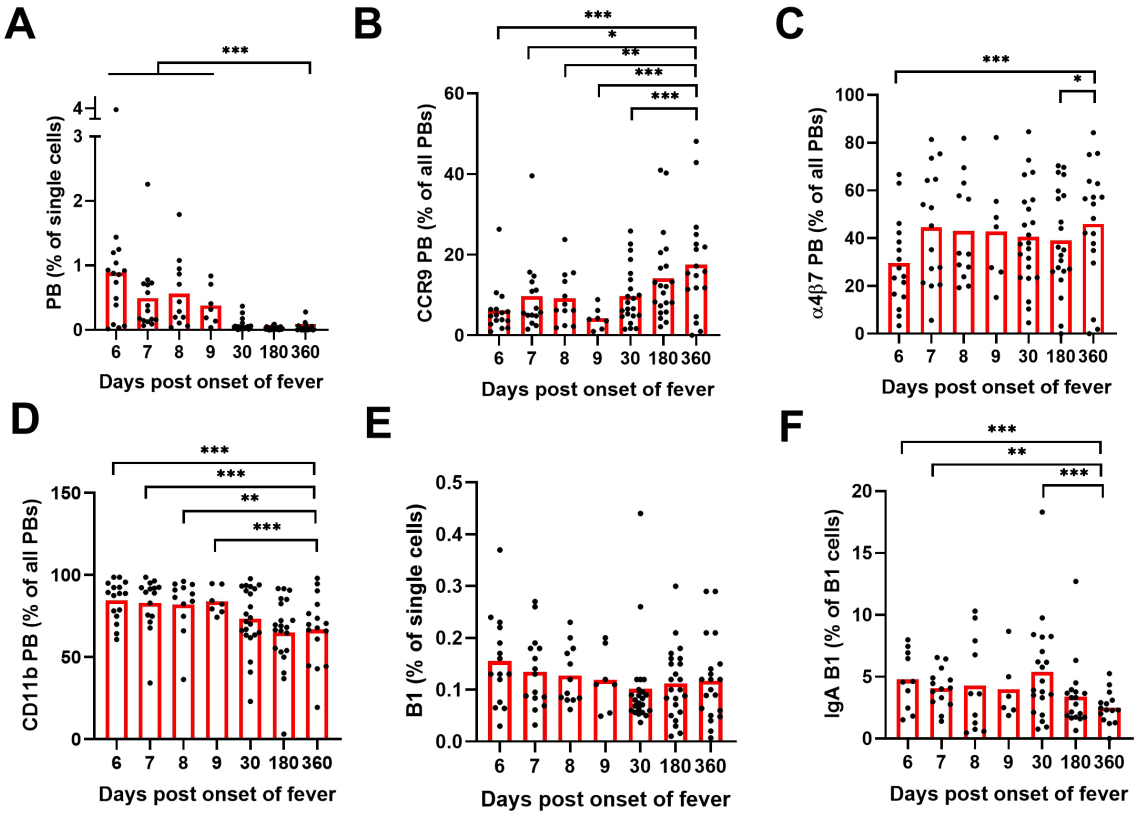

FIGURE 1
Multiparameter flow cytometric analysis of PBs and B1 cells in peripheral blood of PUUV-HFRS. PBMCs from hospitalized (days 6-9 after onset of fever, n = 7-16 per day), two weeks after discharge (~30 days post onset fever, n = 23) and recovered (180 and 360 days post-onset of fever, n =21-23) patients (total n = 25) were stained with a panel of fluorochrome-labeled antibodies and live/dead green viability stain. Stained cells were analyzed by flow cytometry. **(A)** The frequencies of plasmablasts (PBs) in all single cells. **(B)** The frequencies of PBs expressing cell surface CCR9. **(C)** The frequencies of PBs expressing cell surface integrin α4β7. **(D)** The frequencies of PBs expressing cell surface integrin CD11b. **(E)** The frequencies of B1 cells in all single cells. **(F)** The frequencies of surface IgA expressing B1 cells out of all B1 cells. Statistical significance at each time point as compared to recovery at 360 days post-onset of fever were assessed by generalized estimating equations. ***, ** and * indicate p-values <0.001, < 0.01 and < 0.05, respectively.

In agreement with our previous findings, we observed a significant increase (at least 10-fold) in PB frequencies during acute PUUV-HFRS as compared to recovery stage samples collected 360 days after fever onset (R360), which represented healthy steady state (Figure 1A). Interestingly, a significantly diminished proportion of PBs expressed CCR9 during acute PUUV-HFRS as compared to steady state (Figure 1B), and the frequencies of α4β7 expressing PBs were also reduced at 6 days after onset of fever (aof) (Figure 1C). In contrast, the proportion of CD11b-expressing PBs significantly increased during acute PUUV-HFRS (Figure 1D). Of all the PBs detected during the acute stage approximately 20-30% expressed surface IgA, while steady state samples demonstrated over 30% surface IgA expression (Supplementary Figure 2A). We previously observed that ~50% of acute PUUV infection-associated PBs expressed intracellular IgA (17), which together with the current findings indicated that a significant proportion of IgA PBs did not express surface-bound IgA. Compared to all PBs, the observed trends in the expression of α4β7 and CD11b in IgA PBs were comparable, showing diminished early α4β7 expression and significantly elevated CD11b expression in acute PUUV-HFRS (Supplementary Figures 2B–D). However, the frequencies of IgA-expressing PBs were too low for a robust comparison of differences in CCR9 expression between the time points.

The frequencies of the putative mucosal-associated B1 cells did not significantly alter during the course of PUUV-HFRS (Figure 1E). Strikingly however, significantly more of the identifiedB1 cells expressed surface IgA in acute and postacute stages as compared to recovery (approximately 5% expressed surface IgA at acute stage, Figure 1F). The mucosal homing receptor expressions of α4β7, CD11b, and CCR9 remained unaltered in B1 cells during acute stage as compared to recovery (Supplementary Figures 2E, F), although a slight increase in CCR9 expression was observed at postacute stage. For IgA B1s, the cell frequencies were too low for reliable comparisons.

IgA ASCs produce mucosal-like IgA during acute PUUV-HFRS

Mucosal IgA is typically polyreactive. To assess the polyreactivity of the IgA produced by the ASCs of the peripheral

10.3389/fimmu.2024.1480041

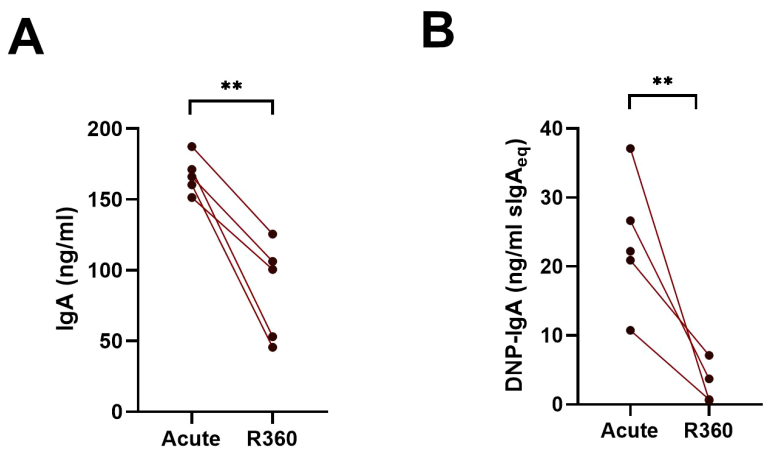

FIGURE 2
Cells in the peripheral blood spontaneously produce polyreactive IgA during acute PUUV-HFRS. PBMCs isolated from acute (1st day of hospitalization, n = 5) or recovery (360 days post-onset of fever; R360, n = 5) of PUUV-HFRS were cultured for 6 days and supernatants analyzed for total IgA **(A)** and DNP-reactive IgA **(B)** by ELISA. Salivary sIgA was used as standard in **(B)** and concentrations reported as sIgA equivalent. The lines connect matched data obtained from the same patient. Statistically significant differences between groups were assessed by paired samples T-test. ** indicate p-values <0.01.

blood of PUUV-HFRS patients, we cultured PBMCs obtained from patients in acute (1st day of hospitalization) or recovery stage (R360) of the disease for 6 days and analyzed the supernatants for IgA production by ELISA. We utilized a previously established method to assess antibody polyreactivity by measuring its ability to bind dinitrophenol (DNP)-conjugated albumin (21) using salivary sIgA as the reference. Consistent with the significantly increased levels of IgA ASCs in acute PUUV-HFRS, we observed markedly higher total IgA production from PBMCs at acute HFRS vs. R360 (Figure 2A). Interestingly, a notable fraction (~10-20% estimated using sIgA as a reference) of the IgA produced by PBMCs from the acute stage bound DNP (Figure 2B), suggesting substantial polyreactivity in the IgA response during acute PUUV-HFRS.

Increased levels of circulating polyreactive IgA, virus-specific IgA and sIgA in acute PUUV-HFRS

To understand the changes in the composition of circulating IgA during acute PUUV-HFRS, we analyzed sequential serum samples collected during acute PUUV-HFRS (days 5-9 aof), at postacute stage two weeks after discharge (~30 d aof), and at recovery 180 d and 360 d aof. The total IgA levels did not show significant variation across the time points (Figure 3A), whereas DNP-reactive IgA was significantly increased during acute illness (5-9 d aof) and remained elevated two weeks after discharge (~30 d aof) as compared to full recovery at R360 (Figure 3B). As expected, samples collected during acute illness (5-9 d aof) and in the postacute stage (30 d aof) showed significantly higher virus-specific IgA levels (using PUUV N protein as the antigen) as compared to samples collected following full recovery at R180 and R360 (Figure 3C).

To further assess the mucosal-like characteristics of the circulating IgA, we developed an ELISA to detect IgA complexed with secretory component (SC), indicative of sIgA. We found significantly increased levels of sIgA in the samples collected in acute phase as compared to those collected in recovery phase of the disease (Figure 3D)., Our findings are indicative of a mucosal-like systemic IgA response in the circulation during acute PUUV-HFRS.

IgA autoantibodies to endothelial cells are increased during acute PUUV-HFRS

Endothelial cells (ECs) are the primary target of hantavirus infection, but direct infection of ECs does not typically compromise the monolayer integrity. Therefore, it appears likely that immunological mechanisms contribute to EC permeability and disease progression during HFRS (3, 4). We aimed to assess whether circulating IgA could contribute to vascular pathology by binding to infected and/or non-infected ECs during PUUV-HFRS. Patient serum obtained at the first day of hospitalization (acute) or at full recovery (R360) was incubated with PUUV-infected (nearly 100% infection, as shown in Figure 4A) vs. non-infected (mock) blood microvascular endothelial cells (BECs). After washing, the levels of cell-bound IgA were analyzed by on-cell ELISA. We observed significantly increased IgA binding to both PUUV-infected and mock-infected BECs in acute PUUV-HFRS as compared to R360 (Figure 4B). Consistent with the presence of virus-specific IgA, the serum obtained from the acute phase showed enhanced binding to infected as compared to mock-infected BECs. The binding of acute-phase IgA to non-infected BECs (in the absence of viral antigen) may be attributed to the previously observed polyreactive nature of IgA, suggesting a virus-independent IgA-mediated immune response towards ECs. This

10.3389/fimmu.2024.1480041

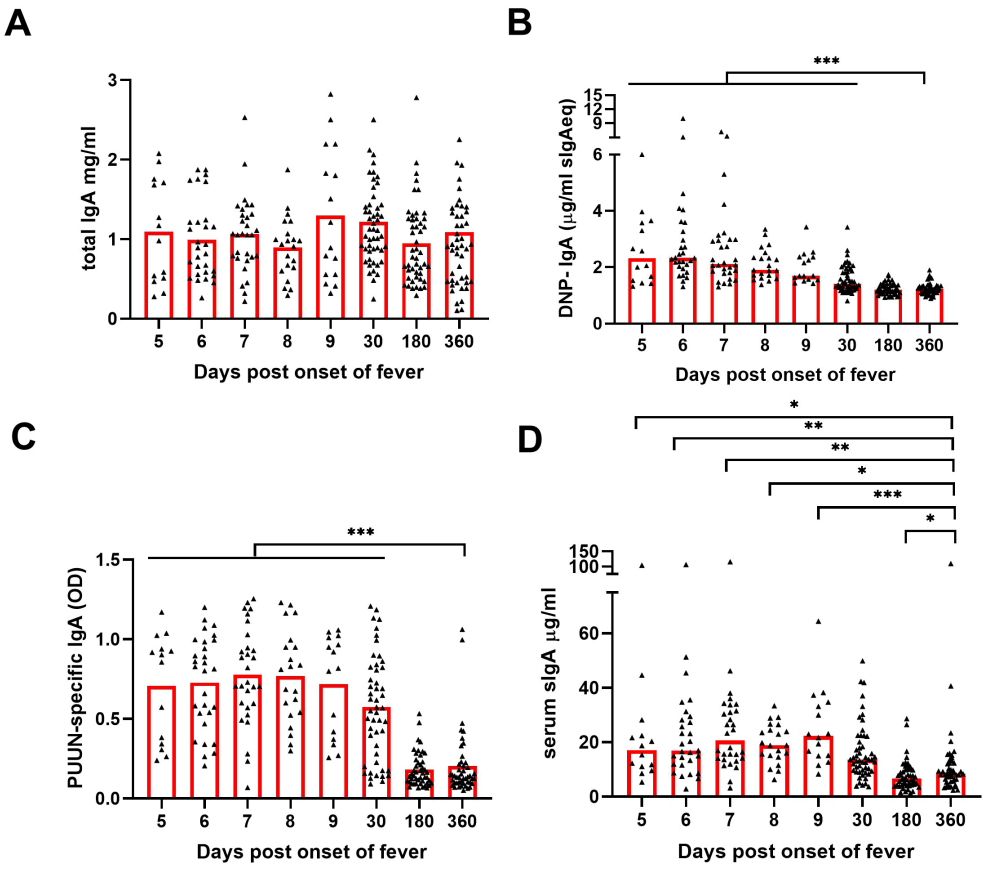

FIGURE 3
Increased levels of circulating polyreactive, PUUN-specific and secretory IgA in acute PUUV-HFRS. Sequential serum samples from hospitalized (days 5-9 post onset of fever, n = 14-30 per day), two weeks after discharge (~30 days post onset fever, n = 51) and recovered (180 and 360 days post-onset of fever, n = 47-48) PUUV-HFRS patients (total n = 55) were analyzed for total IgA **(A)**, DNP-reactive IgA **(B)**, PUUN-specific IgA **(C)** as well as for secretory IgA **(D)** by ELISA. Statistically significant differences at each time point as compared to recovery at R360 were assessed by generalized estimating equations. OD = optical density at 450 nm. ***, ** and * indicate p-values <0.001, <0.01 and <0.05, respectively.

phenomenon could potentially be a contributing factor to the increased EC permeability observed during HFRS.

Increased circulating sIgA, virus-specific IgA and frequencies of the putative IgA B1 cells increase with worsened kidney injury

In addition to vascular permeability, the hallmarks of PUUV-HFRS include AKI, the extent of which can be indirectly assessed by measuring blood creatinine levels (22). We stratified the patients based the maximum blood creatinine levels measured during hospitalization as having a mild (blood creatinine ≤ 265 µmol/L, AKI stage 2 or lower) or severe (> 265 µmol/L; AKI stage 3) PUUV-HFRS. Our analyses revealed that the patients with severe illness had higher levels of sIgA, PUUN-specific IgA and the putative IgA B1 cells, whereas the total IgA, DNP IgA, IgA AECA or PBs (Figures 5A–E and Supplementary Figures 3A–C) did not demonstrate statistically significant differences between the groups. These findings suggest that mucosal and virus-specific IgA responses might play a role in the development of AKI, while IgA polyreactivity *per se* would not. Due to its potential role in vascular pathology, we also stratified patients based on the severity of thrombocytopenia (TC, severe TC with platelet count nadir <50 $*10^4$/µl blood). However, none of the analyzed parameters were significantly increased or decreased in patients with lower platelet counts (Figures 5F–H and Supplementary Figures 3D–H).

The polyreactivity and virus neutralization ability of PUUV-induced IgA associates with its multimericity

Secretory IgA appears mostly as dimers (dIgA) but also as higher order complexes (polymeric IgA, pIgA). To understand further the nature of the IgA response and its molecular complexity, we isolated total IgA from acute (1^{st} day of hospitalization) vs. recovery (R360) PUUV-HFRS (patient matched samples, n = 6-7) and separated the monomeric (mIgA), dimeric (dIgA) and polymeric (pIgA) IgA forms by size-exclusion chromatography (a representative chromatogram and western blot of IgA fractions are shown in Supplementary Figures 4A, B). Interestingly, when normalized to mIgA we observed increased levels of dIgA and pIgA in acute vs. R360 samples (Figure 6A). The

10.3389/fimmu.2024.1480041

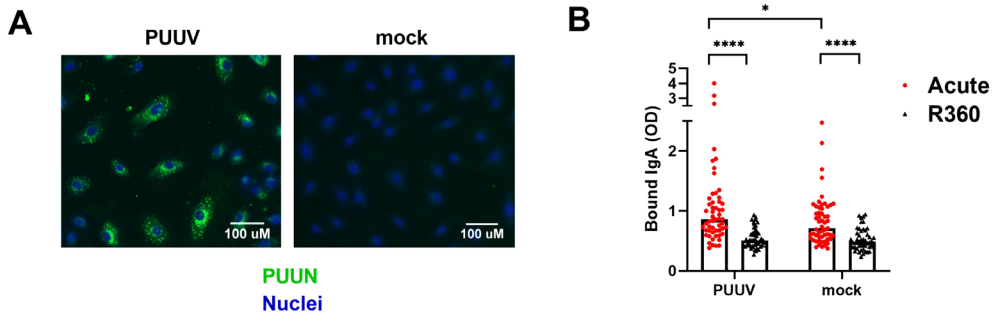

FIGURE 4
Circulating IgA during acute PUUV-HFRS binds microvascular endothelial cells. PUUV- or mock-infected primary blood microvascular endothelial cells (BECs) were fixed at 24 h post-inoculation and used for studying the IgA responses of acute- and recovery-phase sera. **(A)** An overlay of immunofluorescence for PUUN (green)- and Hoechst33342 (blue)-stained PUUV- and mock-infected BECs without the addition of patient serum. **(B)** Serum from acute (1st day of hospitalization, n = 55) or recovery (360 d post onset of fever, R360, n =48) PUUV-HFRS was added on PUUV- or mock-infected BECs for 1 h. After washing, cell-surface bound IgA was measured with on-cell ELISA and optical density (OD, at 450nm) recorded. Statistically significant differences between acute and recovery samples were assessed by two-way ANOVA including Tukey's multiple comparison test. **** and * indicate p-values <0.0001 and <0.05, respectively.

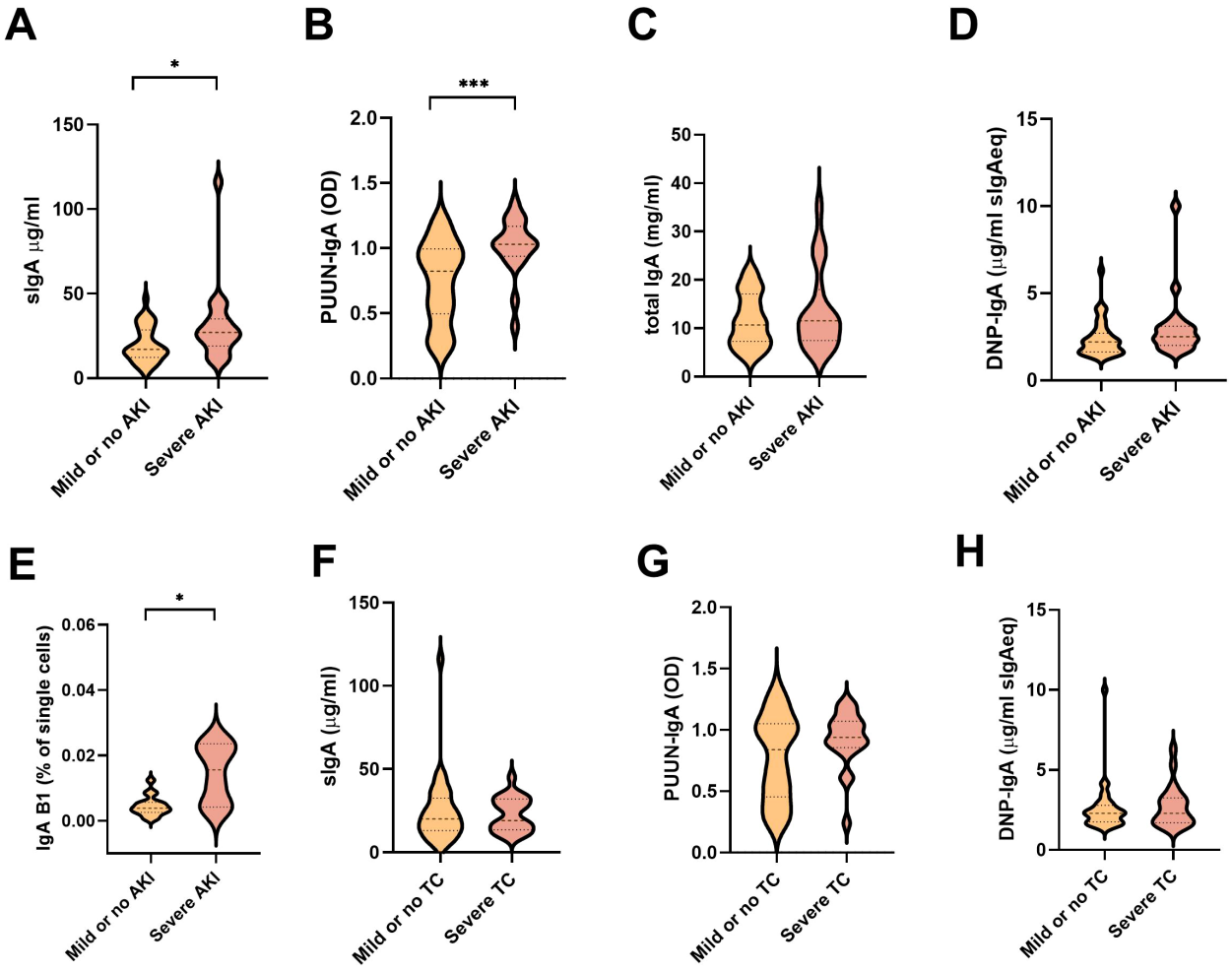

FIGURE 5
Association between measured soluble IgA and IgA ASC levels with parameters of disease severity. **(A–E)** The PUUV-HFRS patients (n = 55) were stratified based the maximum blood creatinine levels measured during hospitalization as mild (blood creatinine ≤ 265 µmol/l = AKI stage 2 or lower, n = 36) or severe (blood creatinine > 265 µmol/l = AKI stage 3, n = 19) or **(F–H)** minimum thrombocyte levels as mild or no thrombocytopenia (TC, ≥ 50 * 10^4/µl blood, = 33) and severe TC (< 50 * 10^4/µl blood, n = 21). The maximum levels of sIgA **(A, F)**, PUUN-specific IgA **(B, G)** DNP-reactive IgA **(C, H)**, total IgA **(D)**, and IgA B1 cells **(E)** measured during hospitalization were grouped based on patient severity criteria and significant differences assessed by Mann-Whitney test. *** and * respectively indicate p-values <0.001 and <0.05.

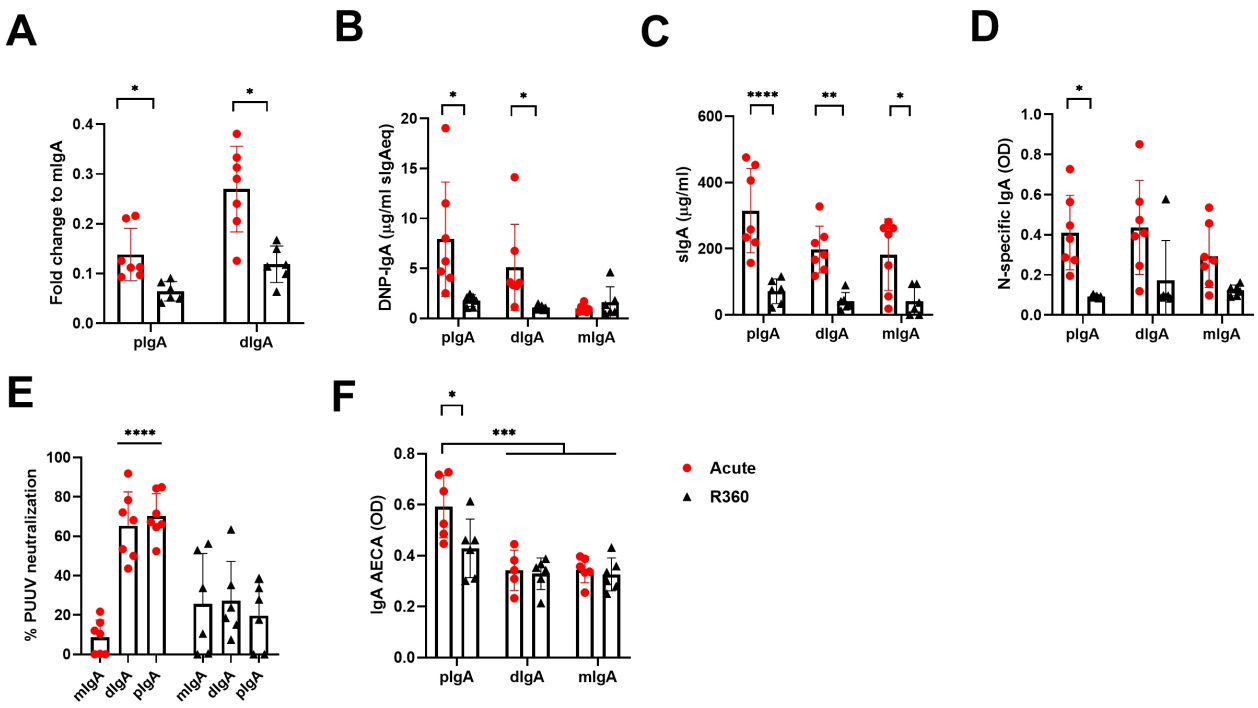

FIGURE 6
Increased levels of circulating multimeric IgA in acute PUUV-HFRS. Total IgA was isolated from serum of acute (1st day of hospitalization, n = 7) or recovery (360 d post onset of fever, R360, n = 6) PUUV-HFRS by Peptide M followed by size −exclusion chromatography to separate polymeric, dimeric and monomeric forms of IgA. Isolated IgA fractions were analyzed for fold change of total IgA concentration compared to mIgA **(A)**. After normalization, IgA fractions were analyzed for DNP-reactive IgA **(B)**, sIgA **(C)**, PUUN-specific IgA **(D)** and IgA AECAs **(F)**. The neutralization of PUUV was analyzed by a microneutralization test **(E)**. OD = optical density at 450nm. Statistically significant differences between acute and recovery samples of each fraction were assessed by two-way ANOVA including Tukey's multiple comparison test. ****, ***, ** and * indicate p-values <0.0001, < 0.001, <0.01 and <0.05, respectively.

mIgA levels were comparable between groups (Supplementary Figure 4C). Thus, multimeric IgA (dIgA and pIgA combined) was approximately 40% of all circulating IgA in acute PUUV-HFRS when compared to 20% at steady state (R360).

Interestingly, the pIgA and dIgA fractions showed significantly increased polyreactivity and elevated levels of sIgA as compared to recovery phase samples or their mIgA counterparts isolated from the same samples (Figures 6B, C). However, unexpectedly, increased levels of sIgA were found also mIgA fraction of acute disease (Figure 6C), possibly indicating breakdown of IgA complexes, while antigen specificity was evenly spread between IgA fractions from acute stage (Figure 6D). In striking contrast to the latter, PUUV microneutralization assays indicated that pIgA and dIgA, but not mIgA, neutralized virus in cell culture (Figure 6E). This suggests that efficient virus neutralization requires multimeric IgA. Interestingly, acute pIgA fractions showed elevated EC binding ability as compared to acute dIgA or mIgA, indicating that PUUV-induced IgA AECAs are polymeric (Figure 6F).

Multimeric IgAs form stable complexes with CD89

IgA exerts its effector functions mainly through the IgA receptor CD89. To understand whether the multimericity of IgA in PUUV-HFRS could affect its effector functions, we analyzed the binding kinetics of different IgA fractions to CD89. The isolated IgAs from different donors, as described above, were pooled together in equal ratios and used as analytes in a surface plasmon resonance (SPR) assay, with a CD89-coated surface as the ligand. The kinetic constants were obtained by fitting obtained sensorgrams to a Langmuir model assuming 1:1 binding stoichiometry. All IgA fractions were able to bind to CD89, with mIgA showing strongest apparent dissociation constant Kd_{app} compared to dIgA or pIgA (Table 4 and Figures 7A–C). However, when comparing the affinity rate constants, markedly differing binding kinetics between different IgA fractions were observed. Polymeric IgA exhibited significantly reduced dissociation rates compared to dIgA and mIgA, with mIgA having the highest dissociation rate. This indicated that the complexes formed between dIgA or pIgA and CD89 are more stable compared to those formed by mIgA. On the other hand, mIgA showed significantly increased association rates compared to multimeric IgAs, which translated to its increased overall affinity towards CD89. When comparing IgAs from acute vs. R360 stages of PUUV-HFRS, no significant differences were observed for any IgA fraction (Table 4 and Supplementary Figures 5A–C).

To confirm the observed differences using pooled IgA fractions, we set up an ELISA assay to analyze the binding of individual patient IgAs to CD89-coated plates. This assay allowed us to

TABLE 4 Apparent kinetic affinity constants between IgA fractions and the IgA receptor CD89.

IgA fraction	Kd_{app} (mol/L)	ka_{app} (mol/L/s)	kd_{app} (1/s)
acute mIgA	$2.05*10^{-8}$	$2.08*10^{5}$	$4.25*10^{-3}$
acute dIgA	$9.75*10^{-7}$	$1.12*10^{3}$	$1.09*10^{-3}$
acute pIgA	$2.23*10^{-7}$	$3.44*10^{3}$	$7.68*10^{-4}$
R360 mIgA	$3.44*10^{-8}$	$1.16*10^{5}$	$4.00*10^{-3}$
R360 dIgA	$4.13*10^{-7}$	$2.88*10^{3}$	$1.19*10^{-3}$
R360 pIgA	$2.20*10^{-7}$	$4.21*10^{3}$	$9.26*10^{-4}$

Apparent affinity constants were assessed using langmuir 1:1 binding model by globally fitting sensorgrams obtained after running various IgA concentrations on a CD89-coated sensor chip as depicted in Figures 7A–C and Supplementary Figures 5A–C.

measure IgA-CD89 interactions in the presence of the previously identified antigens PUUN and DNP-albumin. Interestingly, compared to dIgA or mIgA, pIgA showed significantly increased binding to CD89, while the presence of excess amounts of antigen did not significantly alter the interaction efficiency in this assay (Figure 7G). These findings suggest that the increased stability of pIgA-CD89 interaction, as observed by the kinetic analysis using SPR, plays a major role in the outcome of this ELISA assay. However, the presence of antigen did not impact IgA binding to CD89, indicating that the interaction is mediated by the Fc portion of IgA, as expected. Similarly to the SPR analysis, no significant differences were observed between IgAs isolated from the acute vs. R360 phases in the ELISA (Figure 7E).

pIgA activates neutrophils

The IgA receptor CD89 is widely expressed in neutrophils, which suggests that neutrophils could play a key role in sensing changes in the IgA composition during PUUV-HFRS. We therefore analyzed whether the isolated IgA fractions could mediate neutrophil responses. We isolated neutrophils from healthy volunteers and incubated the isolated neutrophils with different IgA fractions for 4-hr before being analyzed for reactive oxygen species (ROS) generation and expression of surface markers LOX-1, CD66b, CD11b, CD62L and HLA-DR by flow cytometry.

Indeed, irrespective of the sampling time point (acute or R360), the pIgA differed significantly from dIgA or mIgA in its ability to induce increased frequencies of ROS producing as well as LOX-1 and high CD66b expressing neutrophils (Figures 8A–C, representative histograms shown in Supplementary Figure 6). Furthermore, the pIgA-treated neutrophils displayed lower frequency of CD62L expression (Figure 8D) and increased expression of CD11b and HLA-DR as judged by elevated MFI (Figures 8E, F). Collectively, these data indicate that pIgA activates pro-inflammatory responses in neutrophils, which could be linked to its ability to form stable complexes with CD89. Importantly, the pro-inflammatory effect of pIgA did not significantly differ between acute vs. R360 of PUUV-HFRS, suggesting that it is an intrinsic characteristic of pIgA and not directly related to acute disease. However, due to the significantly increased levels of pIgA in acute PUUV-HFRS it is likely that net pro-inflammatory effect of pIgA is significantly elevated as compared to steady state.

Discussion

The pathogenesis of HFRS is mediated by an exacerbated immune response to the causative virus (5). The early phase of orthohantavirus infections in humans remains unclear, but since it is acquired through inhalation from rodent excreta, the virus must initially make contact with host mucosal compartments. However, the role of mucosal immunity in hantavirus-mediated diseases remains obscure. Mucosal immunity is largely mediated by IgA, which, given the large mucosal surface area, is the most abundant immunoglobulin in humans. Previous reports indicate that circulating IgA responses are elevated in acute PUUV-HFRS (23) and that a majority of PBs induced by orthohantavirus infection express IgA in both in HCPS and HFRS (17, 24). These findings imply that the mucosal immune compartment is activated by orthohantavirus infection, but the exact type of induced IgA and its role in disease progression are not well understood.

In this study, we analyzed the IgA-expressing cellular landscape in the periphery in more detail. In addition to the IgA PBs previously described, we found that circulating putative IgA-expressing B1 cells are also significantly increased. Consistent with the upregulation of peripheral IgA ASCs, we detected increased levels of polyreactive and secretory IgA in blood of patients. Notably, the levels of sIgA were increased with worsened AKI, a hallmark of HFRS. Furthermore, we found that infection-induced IgA interacts with endothelial cells and circulates as multimeric complexes, which strongly associated with the IgA receptor CD89 and induced pro-inflammatory responses in neutrophils. These results suggest a model in which PUUV infection could induce pro-inflammatory mucosal-like IgA responses in the periphery, potentially contributing to the disease progression of PUUV-HFRS.

Plasma cell trafficking is mediated by adhesion molecules and chemokine receptors (10). The integrins α4β7 and α4β1 respectively mediate the migration of plasma cells and PBs to the intestine and non-intestinal sites, such as the respiratory tract. Additionally, intestinal IgA plasma cells are characterized by CD11b expression (12) while CCR9 directs cells specifically to the small intestine (11). In the current study, we investigated the surface expression of α4β7, CD11b and CCR9 in infection-induced PBs to better understand their migratory patterns in mucosal versus systemic compartments. Since plasma cells in the steady state express high levels of the intestinal homing receptor α4β7 (25) they serve as a reference phenotype for intestinal PBs. We found that infection-induced PBs displayed significantly less CCR9 expression throughout the acute phase (hospitalization), while α4β7 was also downregulated at the early time point compared to PBs in the patient-matched recovered steady state. In contrast, CD11b expression was strongly elevated in acute PBs. Thus, our findings suggest that infection-induced PBs are distinct from the typical mucosal PBs and, based on their low CCR9 expression, are

10.3389/fimmu.2024.1480041

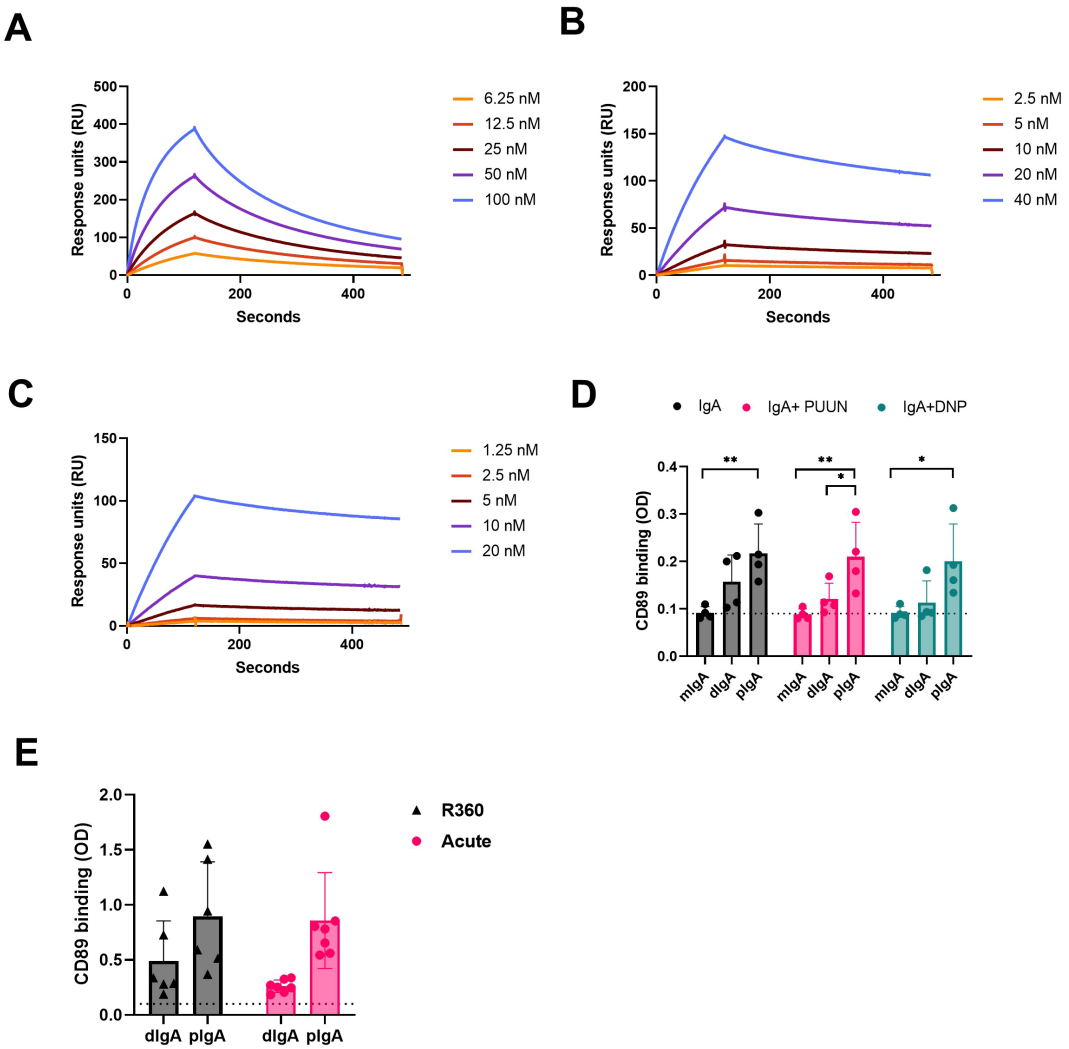

FIGURE 7
CD89 receptor binding kinetics of circulating mIgA, dIgA and pIgA. **(A–C)** Surface plasmon resonance (SPR) binding kinetics assay using Biacore T100. The IgA receptor CD89 was coated on the sensor chip surface, and different IgA fractions isolated from acute PUUV-HFRS (n = 7) were pooled in equal ratio and used at indicated concentrations: **(A)** monomeric IgA (mIgA), **(B)** dimeric IgA (dIgA) and **(C)** polymeric IgA (pIgA). **(D)** CD89 was coated on an ELISA plate, and binding of mIgA, dIgA and pIgA from acute PUUV-HFRS (n = 4) was analyzed. The binding assays were performed in the presence of 100-fold excess PUUN or DNP-albumin where indicated. **(E)** Comparative CD89-binding ELISA was performed with dIgA and pIgA isolated from acute (n = 7) vs. recovery (n = 6) PUUV-HFRS. Dotted lines indicate baseline optical density (OD, 450nm) levels. Statistically significant differences between acute and recovery samples of each fraction were assessed by two-way ANOVA including Tukey's multiple comparison test. ** and * indicate p-values <0.01 and <0.05, respectively.

not targeted to the small intestine but rather could migrate to the site of inflammation. For instance, some PBs could target the kidneys, where we previously observed significant plasma cell infiltration in acute PUUV-HFRS (17). The increased expression of CD11b also supports the intestinal homing of infection-induced PBs and may reflect their vigorous proliferation and increased IgA expression, as previously described for CD11b+ IgA plasma cells over their CD11b- counterparts (12, 26). In light of these findings, we were surprised to detect diminished frequencies of IgA+ PBs in the late acute stage (day 9 aof) compared to the steady state. This could potentially be due to increased IgA secretion by IgA+ PBs, leading to reduced IgA levels expressed on the cell surface.

B cells can be divided into the conventional B cells (B2) and "innate-like" B1 cells. While B2 cells generate specific antibody responses against foreign antigens, typically involving T cell–dependent affinity maturation and somatic hypermutation, B1 cells are predominantly found in the peritoneal and pleural cavities in mice, where they produce natural antibodies, providing a "first line of defense" against infections. B1 cells are relatively poorly studied in humans, with controversy existing regarding the exact phenotype that defines human B1 cells (13). Despite this, due to their residency in mucosal compartments and ability to quickly respond to infections, we were interested in whether these cells could also contribute to mucosal IgA responses during PUUV-HFRS. We defined human B1 cells as $CD20^{+}CD27^{+}CD38^{-/int}CD43^{+}CD70^{-}$ (15) and found significantly elevated circulating levels of surface IgA-expressing B1 cells in acute disease. While it is unclear whether the putative B1 cells identified herein are able to

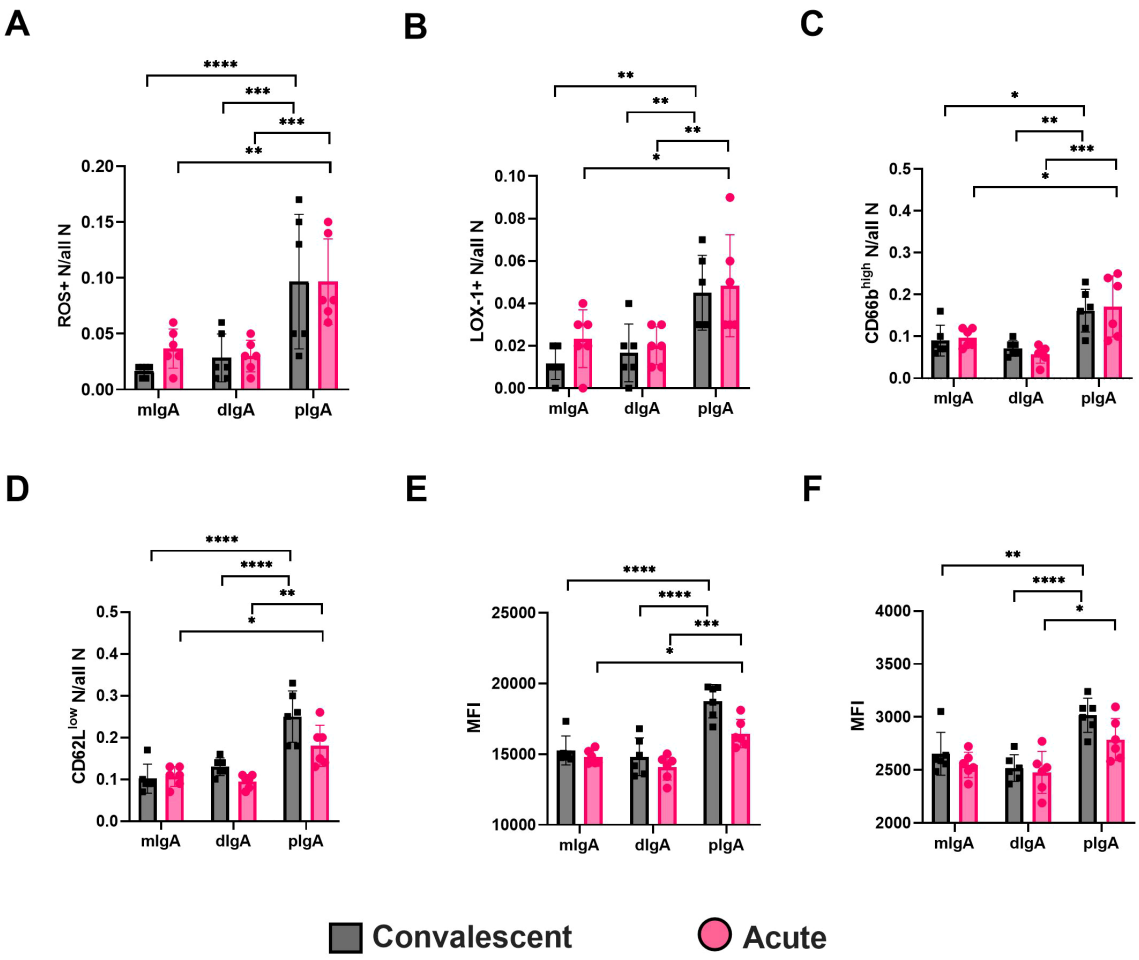

FIGURE 8
Circulating pIgA activates neutrophils. Neutrophils were isolated from healthy volunteers and incubated 4 h with 10 µg/ml of pIgA, dIgA and mIgA obtained from acute (n = 6) vs. recovery (n = 6) PUUV-HFRS patients as previously described. Reactive oxygen species (ROS) generation **(A)** and cell surface expressions of LOX-1 **(B)**, CD66b **(C)**, CD62L **(D)**, CD11b **(E)** and HLA-DR **(F)** were assessed by multicolor flow cytometry. The frequency of gated positive cells **(A–C)**, negative cells **(D)** or median fluorescence intensity (MFI) of all cells **(E, F)** were reported. Statistically significant differences between acute and recovery samples of each fraction were assessed by two-way ANOVA including Tukey's multiple comparison test. ****, ***, ** and * respectively indicate p-values <0.0001, <0.001, <0.01 and <0.05, respectively. The presented data is representative of three similarly performed experiments.

secrete IgA, these findings suggest that, in addition to IgA PBs/plasma cells, B1 cells may also contribute to the total IgA responses during PUUV-HFRS. A large fraction of B1 cells have been described to produce natural IgM antibodies in mice (13). Our study supports the notion that most circulating human B1 cells express IgM, but their frequencies are not similarly upregulated as compared to IgA B1s. Furthermore, we found that a substantial portion of B1 cells expressed α4β7, CD11b and CCR9. However, no changes in the frequencies of these mucosal homing receptors were observed between acute PUUV-HFRS and steady state for total B1 cells. Unfortunately, the low overall low frequencies of IgA B1 cells did not allow for reliable receptor expression comparisons between acute infection and steady state.

We wanted to determine whether the elevated IgA ASCs could significantly contribute to the total circulating IgA pools. Since mucosal IgA is polyreactive, we made use of a previously established method to assess antibody polyreactivity through its binding to DNP. DNP is a synthetic molecule not present in the environment, and individuals are not normally exposed to it. It has been shown previously for IgG that antibodies that bind DNP can be considered polyreactive, and their titer to DNP could serve as an index of polyreactivity (21). Thus, in the current study we applied this approach to measure the polyreactivity of IgA. We observed that *in vitro* cultivated PBMCs from acute PUUV-HFRS spontaneously released significant levels of DNP-reactive IgA, which was strongly elevated along also in the serum of patients with acute disease, alongside the expected virus-specific IgA responses. Further supporting the involvement of mucosal-like IgA responses in acute PUUV-HFRS, we also observed increased levels of sIgA in circulation. sIgA is typically found only in mucosal secretions, to which it enters through transepithelial transport. Thus, the presence of sIgA in the circulation of PUUV-HFRS patients could potentially be explained by a breach of the mucosal layers and leakage of its luminal contents into the periphery. However, further evidence is required to support this hypothesis.

Alterations in the EC permeability are characteristic of the orthohantavirus-mediated diseases, with ECs being the prime target of virus replication. Considering the observed IgA polyreactivity and virus specificity, we assessed whether circulating IgA can bind infected and non-infected ECs. Indeed, we found increased levels of IgA bound to *in vitro* PUUV infected and non-infected ECs compared to IgAs from steady state controls. Since the binding was also observed to non-infected ECs, this suggests that IgA polyreactivity may play role in this phenomenon. Importantly, the presence of IgA AECAs in acute PUUV-HFRS indicates that IgA may play role in the development of HFRS pathogenesis by attracting immune responses towards ECs, which could be a causative factor behind increased EC permeability. Interestingly, mucosal IgA is known for its ability to induce the alternate pathway of complement activation (27), which is significantly induced in PUUV-HFRS (28). Thereby it is plausible that IgA AECAs could induce complement activation on the surface of both infected and non-infected ECs.

Mucosal IgA is predominantly found in dimers (dIgA) but also forms higher order complexes (pIgA). In line with the observed increase in systemic mucosal-like IgA responses, we detected increased levels of circulating dIgA and pIgA in acute PUUV-HFRS. IgA complex formation is known to influence its effector functions by facilitating cross-linking of the IgA receptor CD89 (29). Therefore, we investigated the interaction kinetics between the different IgA forms (mIgA, dIgA and pIgA) and CD89 using surface plasmon resonance technology. Interestingly, both dIgA and pIgA differed significantly from mIgA in their slower affinity rate constants. The differences in the dissociation rates were particularly notable, with pIgA showing the slowest rate followed by dIgA, potentially influencing downstream effector functions by enhancing receptor cross-linking. While previous studies have reported the slower dissociation rate of pIgA over mIgA (30), the slower association rates of dIgA and pIgA observed in this study were unexpected, resulting in an overall stronger binding affinity for mIgA. It is important to mention that although the binding between CD89 and mIgA has been shown to follow 2:1 stoichiometry (31), we reported the apparent affinity based on a 1:1 binding model for simplicity. Interestingly, our ELISA binding experiments between IgA and CD89 reflected the differences determined by their variable dissociation rates (pIgA > dIgA > mIgA), suggesting that the reduced association rate of multimeric IgAs was not a limiting factor in the ELISA assay setup. Importantly, IgAs isolated from the convalescent stage of the disease (R360) showed similar affinities to CD89 as IgAs from acute stage, implying that the observed differences between IgA fractions were indeed due to their variable degrees of intrinsic complexity and not related to their antigen specificity or polyreactivity.

In addition to the known pro-inflammatory effects of multimeric IgA (29), we observed elevated ROS generation and increased expression of LOX-1, CD66b, CD11b and HLA-DR in neutrophils upon stimulation with pIgA, but not with dIgA or mIgA. Similarly, as with its interaction with CD89, the source of pIgA (whether isolated from acute or steady state) did not significantly influence its pro-inflammatory effect, suggesting that it is independent of antigen specificity and rather an intrinsic property of pIgA. While the increased pro-inflammatory effects of pIgA are associated with its slower dissociation rates from CD89, a receptor strongly expressed on neutrophils (29), we cannot exclude the possibility that other receptors may play an accessory role in IgA-mediated effector functions in neutrophils. For instance, the effector functions of sIgA are mediated by its binding to Mac-1 on neutrophils (32).

We investigated the potential impact of circulating IgA-expressing putative B1 cells and soluble IgAs on the clinical severity of PUUV-HFRS by stratifying patients based on two independent factors reflecting disease severity: acute kidney injury (AKI) and thrombocytopenia. Remarkably, patients with severe AKI (stage 3) showed significantly elevated levels of sIgA,PUUN-specific IgA and IgA-expressing B1 cells in circulation. The link between mucosal IgA responses and kidney disease is widely recognized in the case of IgA nephropathy (33). Interestingly, while the pathology of IgA nephropathy has been linked to aberrantly glycosylated IgA, increased sIgA deposits in the kidneys have also been observed (34). Whether similar pathological mechanisms contribute to renal complications in HFRS warrants further investigation. However, the lack of association between the measured parameters levels and severe thrombocytopenia suggests that the IgA response is not related to thrombocytopenia in PUUV-HFRS.

Our findings, demonstrating a robust association between the magnitude of virus-specific IgA response and AKI, align with our previous studies indicating a strong association between circulating antibody light chain levels and kidney dysfunction in PUUV-HFRS (17). This supports the concept of immunologically mediated mechanisms contributing to AKI during PUUV-HFRS. Interestingly, a similar strong association between PUUN-specific IgG levels and AKI was not found (35). Our study also revealed a potential mechanism by which IgA could exacerbate disease progression by triggering pro-inflammatory responses in neutrophils, whether there are elicited on the surfaces of infected and non-infected ECs, or possibly on other cells of the kidney. Our data supports the hypothesis that PUUV infection initiates a strong "mucosal-like" IgA response in the circulation, where its excessive pro-inflammatory effects engage innate immune responses.

Our study has some limitations worth discussing. First, our reliance on blood samples from PUUV-HFRS patients restricted the assessment of mucosal IgA responses solely to systemic circulation. Analyzing the type and specificity of mucosal IgA responses in feces, urine and saliva during acute PUUV-HFRS would provide a more comprehensive understanding of the complete IgA response towards PUUV infection. Secondly, our study does not assess the potentially differing contributions of the two IgA isotypes, IgA1 and IgA2, which are known to possess different mucosal location and effector functions (36). Specifically, IgA2 is known for its increased ability to induce neutrophil extracellular traps, a phenomenon known to take place during PUUV-HFRS (37). Thirdly, our study did not directly address the interplay between IgA polyreactivity and antigen specificity. Understanding whether one IgA clone can simultaneously exhibit antigen-specific, polyreactivity and covalently linked to SC would be beneficial. Fourthly, further characterization of the herein identified putative B1 cells is important to confirm that they undoubtedly represent human B1

cells. For instance, more detailed analysis of their phenotype and antibody secretion profile would greatly enhance our understanding of human B1 cells both in relation to PUUV infections and as a whole. Fifthly, our analysis did not include longitudinal samples from donors without previous exposure to PUUV. Therefore, our analysis does not account for potential temporal fluctuations that may arise during the one-year follow-up period. Finally, while our findings are suggestive of a pathological role for IgA in PUUV-HFRS, further studies are needed to elucidate the precise mechanisms through which IgA contributes to the development of AKI, thrombocytopenia and vascular permeability.

Data availability statement

The raw data supporting the conclusions of this article will be made available by the authors, without undue reservation.

Ethics statement

The studies involving humans were approved by Ethical Committee of Tampere University Hospital. The studies were conducted in accordance with the local legislation and institutional requirements. The participants provided their written informed consent to participate in this study.

Author contributions

LC: Data curation, Formal analysis, Investigation, Methodology, Resources, Supervision, Visualization, Writing – review & editing. CB: Data curation, Formal analysis, Investigation, Methodology, Writing – review & editing. VT: Data curation, Formal analysis, Investigation, Writing – review & editing. SanM: Data curation, Formal analysis, Investigation, Writing – review & editing. OV: Conceptualization, Project administration, Resources, Writing – review & editing. AV: Conceptualization, Funding acquisition, Resources, Writing – review & editing. JH: Conceptualization, Data curation, Methodology, Resources, Writing – review & editing. JT: Conceptualization, Writing – review & editing. SatM: Conceptualization, Project administration, Resources, Writing – review & editing. JM: Conceptualization, Methodology, Resources, Writing – review & editing. TS: Conceptualization, Data curation, Formal analysis, Funding acquisition, Investigation, Methodology, Project administration, Resources, Supervision, Validation, Visualization, Writing – original draft.

Funding

The author(s) declare financial support was received for the research, authorship, and/or publication of this article. Financial support was received from Finnish Cultural Foundation, Pirkanmaa Regional fund and Finnish Kidney Foundation (all for JT).

Conflict of interest

The authors declare that the research was conducted in the absence of any commercial or financial relationships that could be construed as a potential conflict of interest.

Publisher's note

Supplementary material

The Supplementary Material for this article can be found online at: https://www.frontiersin.org/articles/10.3389/fimmu.2024.1480041/full#supplementary-material

SUPPLEMENTARY FIGURE 1
Gating strategy allowing for the identification of PBs and B1 cells in PBMC of PUUV-HFRS patients by flow cytometry. After gating of PBMCs (SSC-H vs. FSC-H), single cells (SSC-H vs. SSC-A) and live cells (excluding also non-B cells expressing CD3, CD14, CD56 and CD66), B cells were identified as positive for either CD19, CD20 or both. PBs were identified as CD20 $\pm$ CD19 +IgD-CD27+CD38++CD43+ cells and B1 cells as CD20+CD27+CD38-/intCD43+CD70-. The cells positive for surface expression of IgA, integrin α4β7, CD11b or CCR9 in PBs and B1 were gated as indicated. Contour plots are shown.

SUPPLEMENTARY FIGURE 2
Multiparameter flow cytometric analysis of IgA PBs and B1 cells in peripheral blood of PUUV-HFRS. PBMCs from hospitalized (days 6-9 post onset of fever, n = 14-30 per day), two weeks after discharge (~30 days post onset fever, n =23) and recovered (180 and 360 days post-onset of fever, n = 21-23) patients (total n = 25) were stained with a panel fluorochrome-labeled antibodies and live/dead green viability stain. Stained cells were analyzed by flow cytometry. **(A)** The frequencies of PBs expressing cell surface IgA. **(B)** The frequencies of IgA PBs expressing surface integrin α4β7. **(C)** The frequencies of IgA PBs expressing surface integrin CD11b. **(D)** The frequencies of B1 cells expressing surface integrin α4β7. **(E)** The frequencies of B1 cells expressing surface CD11b. **(F)** The frequencies of B1 cells expressing surface CCR9. Statistically significant differences at each time point as compared to recovery at 360 days post-onset of fever were assessed by generalized estimating equations. ***, ** and * indicate p-values <0.001, < 0.01 and < 0.05, respectively.

SUPPLEMENTARY FIGURE 3
Association between measured soluble IgA and IgA ASC levels with parameters of disease severity. **(A–C)** The PUUV-HFRS patients (n = 55) were stratified based the maximum blood creatinine levels measured during hospitalization as mild (blood creatinine $\leq$ 265 µmol/l = AKI stage 2 or lower, n = 36) or severe (blood creatinine >265 µmol/l = AKI stage 3, n = 19) or **(D–H)** minimum thrombocyte levels as mild or no thrombocytopenia (TC, $\geq$ 50 * 10^4/µl blood, n = 33) and severe TC (< 50 * 10^4/µl blood, n = 21). The maximum levels of PUUV-EC binding IgA **(A, F)**, IgA AECA **(B, G)**, PBs **(C, F)**, IgA B1 cells **(D)** and total IgA **(E)** measured during hospitalization were grouped based on patient severity criteria and significant differences assessed by Mann-Whitney test.

SUPPLEMENTARY FIGURE 4
Isolation of mIgA, dIgA and pIgA from serum of PUUV-HFRS patients. **(A)** Representative chromatogram of the separation of pIgA, dIgA and mIgA from total IgA isolated from acute (1st day of hospitalization and recovery stage

(R360) of PUUV-HFRS. **(B)** Representative non-reducing western blot indicating the molecular weight of isolated mIgA (~180 kDa), dIgA (~360 kDa) and pIgA (> 360 kDa) fractions. The IgA bands were visualized by a polyclonal anti-kappa light chain antibody followed by IRdye-conjugated secondary antibody. Molecular size was estimated using as molecular weight standard on separate lane. **(C)**. The IgA concentration of isolated IgA fractions from acute (n = 7 and R360 phase (n = 6) of PUUV-HFRS were measured by total IgA ELISA.

SUPPLEMENTARY FIGURE 5
CD89 receptor binding kinetics of circulating mIgA, dIgA and pIgA isolated from convalescent PUUV-HFRS analyzed by surface plasmon resonance. The IgA receptor CD89 was coated on the surface of biacore sensor chip and different IgA fractions, **(A)** mIgA, **(B)** dIgA and **(C)** pIgA, isolated from recovery PUUV-HFRS (360 days post onset of fever, n = 6), pooled at equal ratio, and used at indicated concentrations as analytes in a surface plasmon resonance binding kinetics assay using Biacore T100.

SUPPLEMENTARY FIGURE 6
Representative histograms of pro-inflammatory marker expression in neutrophils. Neutrophils were isolated from healthy volunteers and incubated mIgA, dIgA and pIgA isolated from PUUV-HFRS patient serum at acute (n = 7) vs. recovery stages (n = 6) of the disease. The expression of indicated markers were assessed by flow cytometry and representative histograms of pIgA (solid line with grey area)- vs. mIgA (dotted line with white area)-treated neutrophils are shown. The gating area to select ROS **(A)** and LOX-1 **(B)** positive cells as well as cells with high CD66b expression **(C)** is indicated. The cells with diminished CD62L expression were selected by gating as indicated in **(D)**. The increased expression of CD11b **(E)** and HLA-DR **(F)** were assessed by Median fluorescence intensity (MFI).

References

1. Vial PA, Ferrés M, Vial C, Klingström J, Ahlm C, López R, et al. Hantavirus in humans: a review of clinical aspects and management. *Lancet Infect Dis*. (2023) 23: e371–82. doi: 10.1016/S1473-3099(23)00128-7

2. Vaheri A, Smura T, Vauhkonen H, Hepojoki J, Sironen T, Strandin T, et al. Puumala hantavirus infections show extensive variation in clinical outcome. *Viruses*. (2023) 15(3):805. doi: 10.3390/v15030805

3. Mackow ER, Gavrilovskaya IN. Hantavirus regulation of endothelial cell functions. *Thromb Haemost*. (2009) 102:1030–41. doi: 10.1160/TH09-09-0640

4. Hepojoki J, Vaheri A, Strandin T. The fundamental role of endothelial cells in hantavirus pathogenesis. *Front Microbiol*. (2014) 5:727. doi: 10.3389/fmicb.2014.00727

5. Klingström J, Smed-Sörensen A, Maleki KT, Solà-Riera C, Ahlm C, Björkström NK, et al. Innate and adaptive immune responses against human Puumala virus infection: immunopathogenesis and suggestions for novel treatment strategies for severe hantavirus-associated syndromes. *J Intern Med*. (2019) 285:510–23. doi: 10.1111/joim.12876

6. Perley CC, Brocato RL, Kwilas SA, Daye S, Moreau A, Nichols DK, et al. Three asymptomatic animal infection models of hemorrhagic fever with renal syndrome caused by hantaviruses. *PLoS One*. (2019) 14:e0216700. doi: 10.1371/journal.pone.0216700

7. Sinha D, Yaugel-Novoa M, Waeckel L, Paul S, Longet S. Unmasking the potential of secretory IgA and its pivotal role in protection from respiratory viruses. *Antiviral Res*. (2024) 223:105823. doi: 10.1016/j.antiviral.2024.105823

8. Matsumoto ML. Molecular mechanisms of multimeric assembly of igM and igA. *Annu Rev Immunol*. (2022) 40:221–47. doi: 10.1146/annurev-immunol-101320-123742

9. Bunker JJ, Erickson SA, Flynn TM, Henry C, Koval JC, Meisel M, et al. Natural polyreactive IgA antibodies coat the intestinal microbiota. *Science*. (2017) 358. doi: 10.1126/science.aan6619

10. Kunkel EJ, Butcher EC. Plasma-cell homing. *Nat Rev Immunol*. (2003) 3:822–9. doi: 10.1038/nri1203

11. Hieshima K, Kawasaki Y, Hanamoto H, Nakayama T, Nagakubo D, Kanamaru A, et al. CC chemokine ligands 25 and 28 play essential roles in intestinal extravasation of IgA antibody-secreting cells. *J Immunol*. (2004) 173:3668–75. doi: 10.4049/jimmunol.173.6.3668

12. Kunisawa J, Gohda M, Hashimoto E, Ishikawa I, Higuchi M, Suzuki Y, et al. Microbe-dependent CD11b+ IgA+ plasma cells mediate robust early-phase intestinal IgA responses in mice. *Nat Commun*. (2013) 4:1772. doi: 10.1038/ncomms2718

13. Suchanek O, Clatworthy MR. Homeostatic role of B-1 cells in tissue immunity. *Front Immunol*. (2023) 14:1106294. doi: 10.3389/fimmu.2023.1106294

14. Sanz I, Wei C, Jenks SA, Cashman KS, Tipton C, Woodruff MC, et al. Challenges and opportunities for consistent classification of human B cell and plasma cell populations. *Front Immunol*. (2019) 10:2458. doi: 10.3389/fimmu.2019.02458

15. Quách TD, Rodríguez-Zhurbenko N, Hopkins TJ, Guo X, Hernández AM, Li W, et al. Distinctions among circulating antibody-secreting cell populations, including B-1 cells, in human adult peripheral blood. *J Immunol*. (2016) 196:1060–9. doi: 10.4049/jimmunol.1501843

16. Waffarn EE, Hastey CJ, Dixit N, Soo Choi Y, Cherry S, Kalinke U, et al. Infection-induced type I interferons activate CD11b on B-1 cells for subsequent lymph node accumulation. *Nat Commun*. (2015) 6:8991. doi: 10.1038/ncomms9991

17. Hepojoki J, Cabrera LE, Hepojoki S, Bellomo C, Kareinen L, Andersson LC, et al. Hantavirus infection-induced B cell activation elevates free light chains levels in circulation. *PLoS Pathog*. (2021) 17:e1009843. doi: 10.1371/journal.ppat.1009843

18. Marsman C, Verhoeven D, Koers J, Rispens T, Ten Brinke A, van Ham SM, et al. Optimized protocols for *in-vitro* T-cell-dependent and T-cell-independent activation for B-cell differentiation studies using limited cells. *Front Immunol*. (2022) 13:815449. doi: 10.3389/fimmu.2022.815449

19. Duenas M, Salazar A, Ojeda B, Arana R, Failde I. Generalized Estimating Equations (GEE) to handle missing data and time-dependent variables in longitudinal studies: an application to assess the evolution of Health Related Quality of Life in coronary patients. *Epidemiol Prev*. (2016) 40:116–23.

20. Hanley JA, Negassa A, d. Edwardes MD, Forrester JE. Statistical analysis of correlated data using generalized estimating equations: an orientation. *Am J Epidemiol*. (2003) 157:364–75. doi: 10.1093/aje/kwf215

21. Gunti S, Notkins AL. Polyreactive antibodies: function and quantification. *J Infect Dis*. (2015) 212 Suppl 1:S42–46. doi: 10.1093/infdis/jiu512

22. Lewington A, Kanagasundaram S. Renal Association Clinical Practice Guidelines on acute kidney injury. *Nephron Clin Pract*. (2011) 118 Suppl 1:c349–390. doi: 10.1159/000328075

23. de Carvalho Nicacio C, Björling E, Lundkvist A. Immunoglobulin A responses to Puumala hantavirus. *J Gen Virol*. (2000) 81:1453–61. doi: 10.1099/0022-1317-81-6-1453

24. García M, Iglesias A, Landoni VI, Bellomo C, Bruno A, Córdoba MT, et al. Massive plasmablast response elicited in the acute phase of hantavirus pulmonary syndrome. *Immunology*. (2017) 151:122–35. doi: 10.1111/imm.2017.151.issue-1

25. Mei HE, Yoshida T, Sime W, Hiepe F, Thiele K, Manz RA, et al. Blood-borne human plasma cells in steady state are derived from mucosal immune responses. *Blood*. (2009) 113:2461–9. doi: 10.1182/blood-2008-04-153544

26. Fu Y, Wang Z, Yu B, Lin Y, Huang E, Liu R, et al. Intestinal CD11b(+) B cells ameliorate colitis by secreting immunoglobulin A. *Front Immunol*. (2021) 12:697725. doi: 10.3389/fimmu.2021.697725

27. Hiemstra PS, Gorter A, Stuurman ME, Van Es LA, Daha MR. Activation of the alternative pathway of complement by human serum IgA. *Eur J Immunol*. (1987) 17:321–6. doi: 10.1002/eji.1830170304

28. Sane J, Laine O, Mäkelä S, Paakkala A, Jarva H, Mustonen J, et al. Complement activation in Puumala hantavirus infection correlates with disease severity. *Ann Med*. (2012) 44:468–75. doi: 10.3109/07853890.2011.573500

29. Breedveld A, van Egmond M. IgA and fcαRI: pathological roles and therapeutic opportunities. *Front Immunol*. (2019) 10:553. doi: 10.3389/fimmu.2019.00553

30. Oortwijn BD, Roos A, van der Boog PJ, Klar-Mohamad N, van Remoortere A, Deelder AM, et al. Monomeric and polymeric IgA show a similar association with the myeloid FcalphaRI/CD89. *Mol Immunol*. (2007) 44:966–73. doi: 10.1016/j.molimm.2006.03.014

31. Herr AB, White CL, Milburn C, Wu C, Bjorkman PJ. Bivalent binding of IgA1 to FcalphaRI suggests a mechanism for cytokine activation of IgA phagocytosis. *J Mol Biol*. (2003) 327:645–57. doi: 10.1016/S0022-2836(03)00149-9

32. Van Spriel AB, Leusen JH, Vilé H, Van De Winkel JG. Mac-1 (CD11b/CD18) as accessory molecule for Fc alpha R (CD89) binding of IgA. *J Immunol*. (2002) 169:3831–6. doi: 10.4049/jimmunol.169.7.3831

33. Seikrit C, Pabst O. The immune landscape of IgA induction in the gut. *Semin Immunopathol*. (2021) 43:627–37. doi: 10.1007/s00281-021-00879-4

34. Oortwijn BD, Rastaldi MP, Roos A, Mattinzoli D, Daha MR, van Kooten C. Demonstration of secretory IgA in kidneys of patients with IgA nephropathy. *Nephrol Dial Transplant*. (2007) 22:3191–5. doi: 10.1093/ndt/gfm346

35. Iheozor-Ejiofor R, Vapalahti K, Sironen T, Levanov L, Hepojoki J, Lundkvist Å., et al. Neutralizing antibody titers in hospitalized patients with acute puumala orthohantavirus infection do not associate with disease severity. *Viruses*. (2022) 14 (5):901. doi: 10.3390/v14050901

36. Steffen U, Koeleman CA, Sokolova MV, Bang H, Kleyer A, Rech J, et al. IgA subclasses have different effector functions associated with distinct glycosylation profiles. *Nat Commun*. (2020) 11:120. doi: 10.1038/s41467-019-13992-8

37. Raftery MJ, Lalwani P, Krautkrämer E, Peters T, Scharffetter-Kochanek K, Krüger R, et al. [amp]]beta;2 integrin mediates hantavirus-induced release of neutrophil extracellular traps. *J Exp Med*. (2014) 211:1485–97. doi: 10.1084/jem.20131092